ELSEVIER

Journal of Alloys and Compounds 281 (1998) 241–248

Journal of ALLOYS AND COMPOUNDS

# Phase equilibria in the ternary Ga–Pt–Sb system

Klaus W. Richter, Herbert Ipser*

*Institut für Anorganische Chemie, Universität Wien, Währingerstr. 42, A-1090 Vienna, Austria*

Received 26 June 1998

**Abstract**

The phase relationships of GaSb in the ternary system Ga–Pt–Sb were studied within an isothermal section at 500°C by means of X-ray diffraction (XRD) and electron probe micro analyses (EPMA). Ternary phase reactions were determined using differential thermal analyses (DTA) in the platinum-poor area of the phase diagram. All experimental phase diagram data were combined to construct a complete reaction scheme (Scheil diagram) in the investigated composition area and the liquidus surface was derived based on the results of the DTA measurements. 

*Keywords:* Phase diagram; Ga–Pt–Sb system; Thermal analysis; X-ray diffraction; Electron probe microanalysis

## 1. Introduction

The problem of suitable ohmic contacts for III–V semiconductors has been investigated extensively over the last two decades from different points of view (e.g. [1–4]). Since processing of semiconductor devices normally includes exposure to elevated temperatures, interface reactions often occur during the metallization step and further heat treatments. In order to understand these reactions, a thorough knowledge of the phase diagrams formed by the involved elements, i.e. the ternary diagrams of the transition metals under consideration with elements of group III and V, is essential. Furthermore, as these ternary diagrams show the equilibrium phase relationships of the compound semiconductor with the surrounding binary phases, it is possible to find metallic phases that are in thermodynamic equilibrium with the compound semiconductor and therefore may be promising candidates for contact materials.

In a series of previous investigations, phase equilibria of the compound semiconductors GaSb and InSb with Ni and Pd (as possible contact materials) have been studied and some candidates for contact materials within these ternary systems were found [5–8]. The present investigation of the ternary Ga–Pt–Sb phase diagram which covers the system up to about 50 at.% Pt, including all phase relationships around solid GaSb, is part of this ongoing research project.

*Corresponding author.

## 2. Literature review

The Ga–Sb system was assessed by Ngai et al. [9] based upon available literature data up to 1984. Similar to other III–V systems the stoichiometric compound GaSb is the only intermediate phase within the system. GaSb shows a congruent melting point of 711.7°C and it is surrounded by two eutectic reactions.

A detailed evaluation of the Pt–Sb system was given recently by Itkin and Alcock [10]. Altogether, six intermediate phases have been reported in this system, most of them situated in the platinum-rich side of the phase diagram. In the composition area relevant for the present study, the binary phase diagram is rather simple: pyrite-type $PtSb_2$, which is the only intermediate phase in the antimony-rich part of the phase diagram, exhibits a congruent melting point at 1225°C. Antimony-rich liquid decomposes in a eutectic reaction into $PtSb_2$ and Sb at 626°C.

The phase diagram of the Ga–Pt system is given in Massalski's compilation [11]. In the composition range of interest for the present study, i.e. the gallium-rich part of the phase diagram, the line compounds GaPt, $Ga_3Pt_2$, $Ga_2Pt$, $Ga_7Pt_3$ and $Ga_6Pt$ have been reported in literature. The corresponding phase equilibria were taken from the experimental work by Guex and Feschotte [12]. GaPt shows a congruent melting point at 1104°C, whereas all other compounds listed above decompose in a series of peritectic reactions. Furthermore $Ga_2Pt$ was reported to

0925-8388/98/$ – see front matter 
PII: S0925-8388(98)00745-2

Table 1
Binary invariant phase equilibria relevant for the present study

| Phase Reaction | Temperature (°C) | Composition of the involved phases (at.%) | | Literature |
|---|---|---|---|---|
| Congruent: L⇌GaSb | 711.7 | L: 50% Sb | GaSb: 50% Sb | [9] |
| Eutectic: L⇌GaSb+Sb | 589.3 | L: 88.2% Sb | GaSb: 50% Sb | Sb: 100% Sb | [9] |
| Eutectic: L⇌GaSb+Ga | 29.77 | L: 0% Sb | GaSb: 50% Sb | Ga: 0% Sb | [9] |
| Congruent: L⇌$PtSb_2$ | 1225 | L: 66.7% Sb | $PtSb_2$: 66,7% Sb | | [10] |
| Eutectic: L⇌$PtSb_2$+Sb | 626 | L: 99% Sb | $PtSb_2$: 66,7% Sb | Sb: 100% Sb | [10] |
| Congruent: L⇌GaPt | 1104 | L: 50% Ga | GaPt: 50% Ga | | [12] |
| Peritectic: L+GaPt⇌$Ga_3Pt_2$ | 937 | L: 66% Ga | GaPt: 50% Ga | $Ga_3Pt_2$: 60% Ga | [12] |
| Peritectic: L+$Ga_3Pt_2$⇌$Ga_2Pt$ | 922 | L: 68% Ga | $Ga_3Pt_2$: 60% Ga | $Ga_2Pt$: 66,7% Ga | [12] |
| Peritectic: L+$Ga_2Pt$⇌$Ga_7Pt_3$ | 822 | L: 79% Ga | $Ga_2Pt$: 66,7% Ga | $Ga_7Pt_3$: 70% Ga | [12] |

decompose in the eutectoid reaction $Ga_2Pt \rightleftharpoons Ga_7Pt_3 + Ga_3Pt_2$ at 153°C.

All binary invariant phase equilibria that are relevant for the present study as well as the crystal structure data of the corresponding binary phases are listed in Tables 1 and 2, respectively.

An isothermal section of the ternary Ga–Pt–Sb system at 500°C was investigated very recently by Markovski et al. [13] using XRD and EPMA methods. No ternary phase was found within this section and the solubility of the third element in the various binary phases was found to be very small, except for $Ga_3Pt_5$ and $GaPt_3$. The results of this investigation [13] are included in Fig. 1. No additional literature data, concerning phase equilibria at different temperatures or invariant reactions in the Ga–Pt–Sb system could be found.

## 3. Experimental

The samples were prepared from antimony lumps (99.99%, ASARCO, South Plainfield, NJ, USA), platinum wire (99.9%, ÖGUSSA, Vienna, Austria) and gallium shot (99.9999%, Alfa Products, Karlsruhe, Germany). Calculated amounts of the pure elements were weighed (±0.05 mg) into quartz glass ampoules that were then sealed under vacuum ($10^{-1}$ Pa). The samples were melted at 1100°C, cooled slowly (0.5 K $min^{-1}$) to 500°C and then annealed at this temperature for 3 weeks. They were quenched in water and the obtained reguli were weighed back to check for any possible mass loss during preparation. Mass losses were found to be less than 0.3 weight percent in all cases.

DTA measurements were carried out in closed and evacuated quartz glass tubes on a DTA 404S/3 (Netzsch, Selb, Germany). A sample mass of approximately 400 mg was used in the experiments, and the heating rate was generally 2 K $min^{-1}$. The Pt/Pt10%Rh thermocouples were standardized at the melting points of high purity Au and Sb. In order to test the reproducibility of the results, the samples were cycled three times over the respective temperature range of the DTA experiment.

Table 2
Crystal structure data for binary phases relevant for the present study

| Phase | Pearson symbol | Space group | Structure type | Reference |
|---|---|---|---|---|
| GaSb | *cF*8 | $F\bar{4}3m$ | SZn (zinc blende) | [14] |
| $PtSb_2$ | *cP*12 | $Pa\bar{3}$ | $FeS_2$ (pyrite) | [15] |
| GaPt | *cP*8 | $P2_13$ | FeSi | [16] |
| $Ga_3Pt_2$ | *hP*5 | $P\bar{3}m1$ | $Al_3Ni_2$ | [16] |
| $Ga_2Pt$ | *cF*12 | $Fm\bar{3}m$ | $CaF_2$ | [17] |
| $Ga_7Pt_3$ | *cI*40 | $Im\bar{3}m$ | $Ge_7Ir_3$ | [18] |

XRD (X-ray powder diffraction, Guinier-Huber technique) was employed to check the phase composition of the various samples used for DTA measurements. The experiments were carried out using Cu Kα radiation and employing an internal standard of high purity Si.

EPMA measurements were carried out on a Cameca SX 100 electron probe using wavelength dispersive spectroscopy (WDS) for quantitative analyses and employing pure platinum and gallium antimonide as standard materials. The measurements were carried out at 20 kV with a beam current of 20 nA. Due to the interference of Ga Kα and Pt Lα lines, Ga Lα and Pt Lβ lines were used for quantitative analyses. Conventional ZAF matrix correction was used to calculate the compositions from the measured X-ray intensities.

## 4. Results and discussion

### 4.1. Isothermal section at 500°C

A total number of 35 ternary samples were studied within the platinum-poor part of the Ga–Pt–Sb system, and their compositions are indicated in Fig. 1. They were prepared and annealed according to the procedure described in the previous section, and their phase compositions were characterized by XRD (Guinier technique). Some selected samples situated in the different two- and three-phase regions were then investigated by EPMA to determine the compositions of the various phases present. The results for 500°C are shown in Fig. 1 together with data for the platinum-rich part of the system by Markovski et al. [13] in order to present the entire isothermal section.

The phase equilibria of Ga–Pt–Sb at 500°C as they were found in the present study are in perfect agreement with

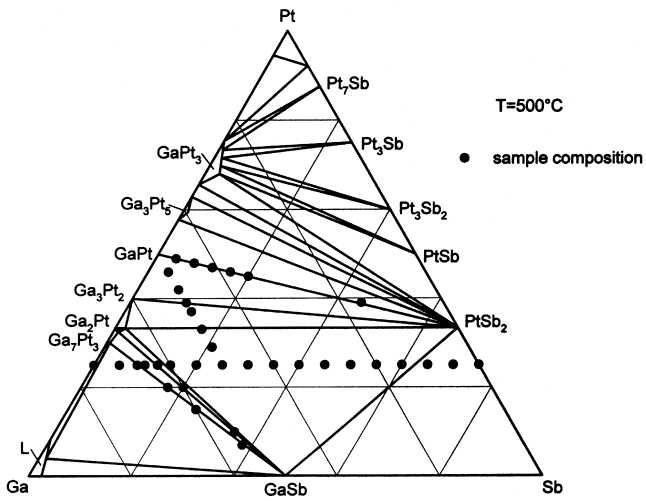


Fig. 1. Isothermal section of Ga–Pt–Sb at 500°C with compositions of investigated samples. Phase equilibria below the section GaPt–$PtSb_2$ are shown according to the present results, those in the platinum rich corner were taken from Ref. [13].

the results of Markovski et al. [13]. As can be seen in Fig. 1, the isothermal section at 500°C appears to be rather simple. The following three-phase regions were identified in the investigated composition range: [L+$Ga_7Pt_3$+GaSb], [$Ga_7Pt_3$+$Ga_2Pt$+GaSb], [$Ga_2Pt$+GaSb+$PtSb_2$], [GaSb+$PtSb_2$+Sb], [$Ga_2Pt$+$PtSb_2$+$Ga_3Pt_2$] and [$PtSb_2$+$Ga_3Pt_2$+GaPt]. EPMA measurements of the samples show, that the two phases $Ga_7Pt_3$ and $Ga_2Pt$ exhibit a small but noticeable homogeneity range towards the ternary system: $Ga_7Pt_3$ was found to dissolve up to 0.6 at.% Sb, $Ga_2Pt$ up to 2 at.% Sb at 500°C (compare Fig. 1). All other phases in the investigated area did not show any significant solubility of the third element.

### *4.2. Ternary phase reactions, series I*

The results of DTA measurements of sample series I are listed in Table 3 together with the interpretation of the various effects. In order to test the reproducibility of the results, the annealed samples were cycled three times over

Table 3
DTA results for Ga–Pt–Sb, series I

| Composition (at.% Ga,Pt,Sb) | Thermal effects (°C) | | | | | | | | |
|---|---|---|---|---|---|---|---|---|---|
| | E | U1 | U2 | U3 | U4 | QBE | Others | Liquidus heating | Liquidus cooling |
| 75, 25, 0 | | | | | | | 820 Binary peritectic | 885 | 871 |
| 69.5, 25, 5.5 | | | | | | | 678(a) 817(b) | 889 | 876 |
| 65, 25, 10 | | | 704 | | | | 804(b) | 896 | 880 |
| 60, 25, 15 | | 686 | | | | | 698(c) | 900 | 874 |
| 55, 25, 20 | | 686 | | | | | 788(d) | 891 | 856 |
| 50, 25, 25 | | 689 | | | | | 841(d) | 889 | 869 |
| 45, 25, 30 | | 686 | | | | | 882(e) | 913 | SC |
| 40, 25, 35 | | 685 | | | | | 879(e) | 945 | SC |
| 35, 25, 40 | | 685 | | | | | 872(e) | 988 | 984 |
| 30, 25, 45 | | 686 | | | | | 868(e) | 1038 | SC |
| 25, 25, 50 | | 686 | | | | | 860(e) | 1069 | 1023 |
| 20, 25, 55 | | 685 | | | | | 849(e) | 1106 | SC |
| 15, 25, 60 | | 686 | | | | | 819(e) | 1137 | 1096 |
| 10, 25, 65 | 588 | | | | | | 686(e) | 1166 | SC |
| 5, 25, 70 | 589 | | | | | | 655(f) | 1195 | 1179 |
| 0, 25, 75 | | | | | | | 631 Binary eutectic | 1224 | 1211 |
| 50, 46, 4 | | | | | 902 | | 983(g) | 1067 | SC |
| 50, 42, 8 | | | | | 902 | | 953(h) | 1001 | SC |
| 50, 39, 11 | | | | | 903 | | | 973 | 962 |
| 50, 37, 13 | | | | 894 | | | | 966 | SC |
| 50, 33, 17 | | 683 | | 892 | | | | 934 | 917 |
| 50, 29, 21 | | 686 | | | | | | 896 | 882 |
| 47, 49, 4 | | | | | | 1033 | | 1083 | SC |
| 44, 48, 8 | | | | | | 1033 | | 1060 | SC |
| 41, 47, 12 | | | | | | 1033 | | – | SC |
| 38, 46, 16 | | | | | | 1034 | | 1052 | 1036 |
| 35, 45, 20 | | | | | | 1031 | | 1069 | 1042 |
| 16, 39, 45 | | | | | | 1028 | | 1176 | 1167 |

SC . . . Strong supercooling, (a) . . . [L+GaSb+$Ga_7Pt_3$]⇌[L+$Ga_7Pt_3$], (b) . . . [L+$Ga_7Pt_3$+$Ga_2Pt$]⇌[L+$Ga_2Pt$], (c) . . . [L+GaSb+$Ga_2Pt$]⇌[L+$Ga_2Pt$], (d) . . . [L+$Ga_2Pt$+$PtSb_2$]⇌[L+$Ga_2Pt$], (e) . . . [L+$Ga_2Pt$+$PtSb_2$]⇌[L+$PtSb_2$], (f) . . . [L+GaSb+$PtSb_2$]⇌[L+$PtSb_2$], (g) . . . [L+GaPt+$PtSb_2$]⇌[L+GaPt], (h) . . . [L+GaPt+$PtSb_2$]⇌[L+$PtSb_2$].

the temperature range between 400°C and the liquidus temperature of the respective sample. For all samples in series I, no significant deviation was found between the thermal effects shown by the original (well annealed) samples and the corresponding effects found in the following cycles. It is therefore estimated, that the applied heating/cooling rate of 2 K $min^{-1}$ was sufficiently low to reestablish equilibrium conditions on cooling. The experimental data listed in Table 3 are the mean values of the thermal effects on heating; in case of the liquidus on cooling, only the highest measured value was listed.

In Fig. 1 the fact that the investigated samples are situated within five different isopleths is shown: in a first series of samples, the two vertical sections at 25 at.% Pt and at 50 at.% Ga, and the section that connects the binary phases [GaPt and $PtSb_2$] were studied by means of DTA. Since it turned out, that difficulties arose in the interpretation of the thermal effects in the region between GaSb, $Ga_7Pt_3$ and $Ga_2Pt$, additional samples were prepared in a second series within the two sections that connect the binary phases [GaSb and $Ga_7Pt_3$] as well as [GaSb and $Ga_2Pt$].

The results of the DTA measurements within the isopleth at 25 at.% Pt, which was selected for a first investigation of ternary phase equilibria, are shown in Fig. 2. Three invariant reactions were found to occur within this section. The ternary eutectic E: [L⇌Sb+$PtSb_2$+GaSb] at 589°C (which seems to be degenerated, i.e. it coincides more or less with the binary eutectic L⇌Sb+GaSb) and the transition reaction U1: [L+$Ga_2Pt$⇌GaSb+$PtSb_2$] at 686°C could be derived directly by combining the DTA results with the information from the isothermal section at 500°. The third invariant reaction, that was found to occur at ca. 700°C at the gallium-rich side of the isopleth, could not be identified without doubt.

The invariant reactions that have to occur in the vicinity of the limiting Ga–Pt system at elevated temperatures could be derived from the isopleth at 50 at.% Ga shown in Fig. 3. Starting from the limiting Ga–Pt system, the two transition reactions U4: [L+GaPt⇌$Ga_3Pt_2$+$PtSb_2$] at 902°C and U3: [L+$Ga_3Pt_2$⇌$Ga_2Pt$+$PtSb_2$] at 894°C could be identified from DTA data. At higher antimony contents the transition reaction U1 at 686°C was found to occur in this section.

The existence of a quasibinary eutectic reaction between the two congruently melting binary compounds $PtSb_2$ and GaPt, which was suggested from the results in the two sections mentioned above, could be proved by DTA experiments within the section GaPt–$PtSb_2$. In Fig. 4 the quasibinary eutectic reaction QBE: [L⇌GaPt+$PtSb_2$] at 1033°C is shown.

Additional EPMA samples were prepared from some of the reguli obtained after DTA measurements, in order to check, whether the phase compositions of these samples are consistent with the proposed phase reactions. It was found, that this is actually true for all invariant phase reactions mentioned above. The EPMA results for the compositions of the various phases were taken as a good approximation of the equilibrium compositions of the phases in the corresponding invariant reaction. The respective values are included in Table 5 that lists the ternary invariant phase reactions. Note, that the solubility of Sb in $Ga_2Pt$ was found to reach 4 at.% at higher temperatures.

### *4.3. Ternary phase reactions, series II*

From the DTA results of series I it was not possible to identify in a definite way the invariant phase equilibria that necessarily have to occur between GaSb, $Ga_7Pt_3$, $Ga_2Pt$ and the liquid phase. The boundary conditions were such

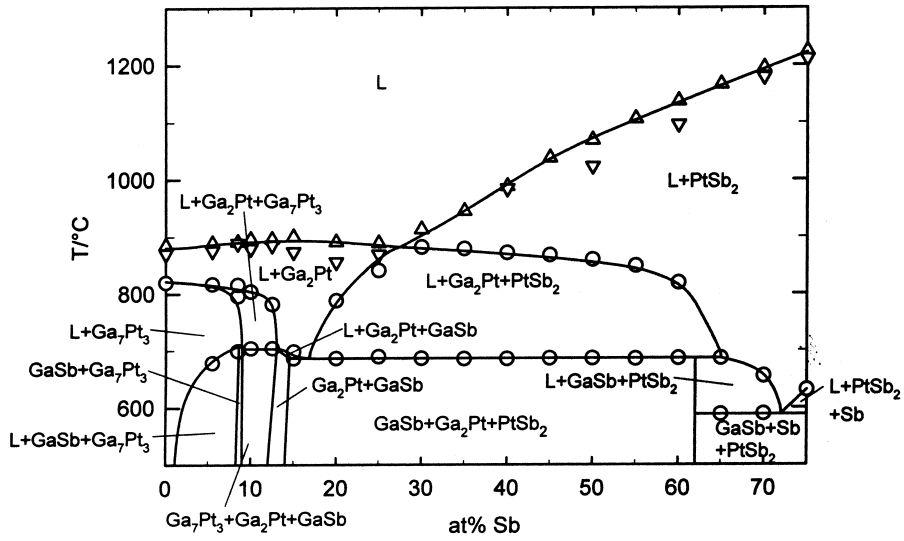


Fig. 2. Vertical section of Ga–Pt–Sb at 25 at.% Pt with experimental data points from DTA (○ ... thermal effect on heating, △ ... liquidus on heating, ▽ ... liquidus on cooling).

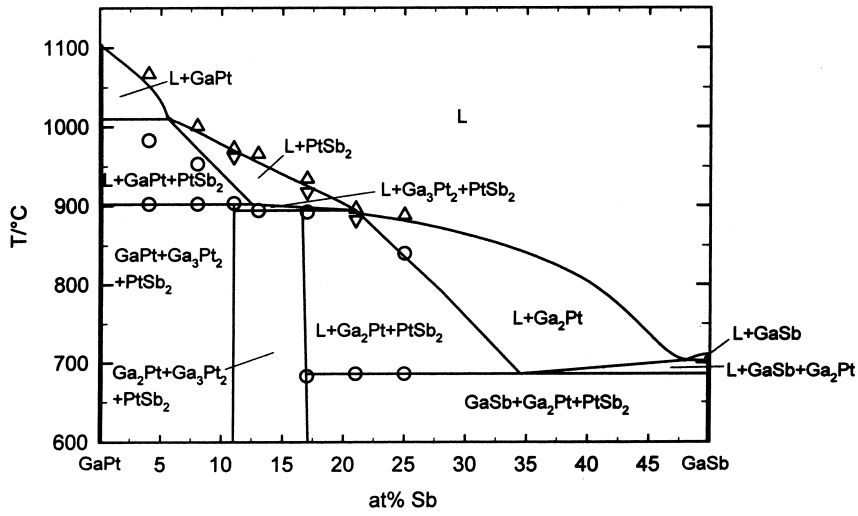


Fig. 3. Vertical section of Ga–Pt–Sb at 50 at.% Ga with experimental data points.

that at higher temperatures a three-phase field [L+$Ga_7Pt_3$+$Ga_2Pt$] exists, whereas at lower temperatures there are three different three-phase fields, [L+$Ga_7Pt_3$+GaSb], [$Ga_7Pt_3$+$Ga_2Pt$+GaSb] and [L+$Ga_2Pt$+GaSb]. Although in the isopleth at 25 at.% Pt thermal effects appear at ca. 700°C in this composition range (see Fig. 2), the only simple phase reaction that could be used to interpret these effects as an invariant reaction in the context of a consistent ternary reaction scheme was the ternary peritectic L+$Ga_2Pt$+$Ga_7Pt_3$⇌GaSb (compare the scheme in Fig. 5a). However, this possibility was excluded due to two facts: First of all, the melting point of binary GaSb is 711.7°C [9], which is definitely higher than the thermal effects found in the DTA experiments. Secondly, the solubility of Pt in GaSb was found to be negligible, both in the present work as well as in Ref. [13].

A careful analysis of the ternary reaction scheme (Scheil flow diagram) resulted in two other consistent possibilities which could explain the reactions occurring between GaSb, $Ga_7Pt_3$, $Ga_2Pt$ and the liquid phase. The first one was a combination of the transition reaction [L+$Ga_2Pt$⇌GaSb+$Ga_7Pt_3$] with a temperature maximum in the three-phase field [L+$Ga_2Pt$+GaSb] (see Fig. 5b), the second one a combination of the transition reaction [L+$Ga_7Pt_3$⇌GaSb+$Ga_2Pt$] with a temperature maximum in the three-phase field [L+$Ga_7Pt_3$+GaSb] (see Fig. 5c). In order to distinguish between the two possible reactions, an additional series of samples (series II) was prepared along the two sections that connect GaSb with $Ga_2Pt$ and $Ga_7Pt_3$, respectively. The experimental results of the corresponding DTA measurements are listed in Table 4.

The DTA data show only a very small difference in the thermal effects of the samples situated in the two different vertical sections. From the fact, that the first reaction temperatures within the section GaSb–$Ga_2Pt$ were found to occur at slightly higher temperatures than in the section

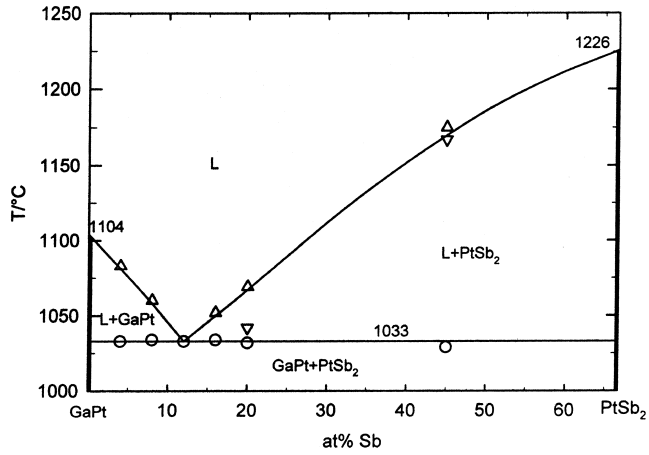


Fig. 4. Quasibinary vertical section between GaPt and $PtSb_2$ with experimental data points.

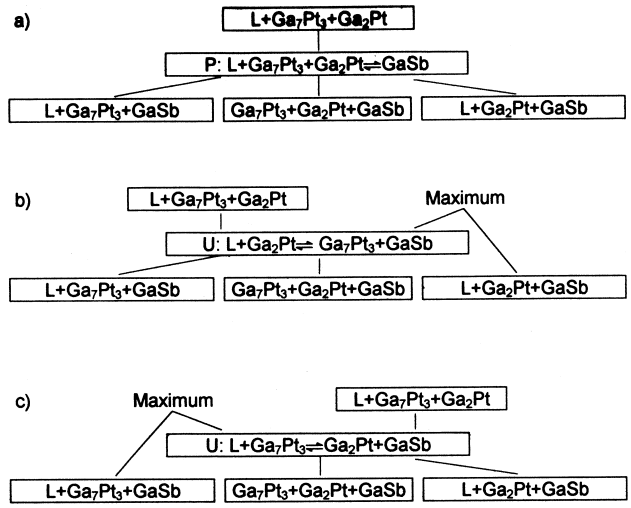


Fig. 5. Three different possible sequences of phase reactions between GaSb, $Ga_2Pt$, $Ga_7Pt_3$ and L (see text).

Table 4
DTA results for Ga–Pt–Sb, series II

| Composition (at.% Ga,Pt,Sb) | Section | Thermal effects (°C) | | | |
|---|---|---|---|---|---|
| | | U2 | Others | Liquidus heating | Liquidus cooling |
| 66.5, 25, 8,5 | $Ga_7Pt_3$–GaSb | | 700(a), 796(b), 816(c) | 894 | 891 |
| 63, 20, 17 | | | 702(a), 781(b), 798(c) | 868 | 871 |
| 60, 15, 25 | | | 702(a), 777(b), 787(c) | 846 | 850 |
| 55, 7, 38 | | | 701(a) | 777 | 754 |
| 62.5,25, 12.5 | $Ga_2Pt$–GaSb | 704 | 781(c) | 896 | 886 |
| 60, 20, 20 | | 704 | 776(c) | 870 | 860 |
| 55, 10, 35 | | 704 | 770(c) | 814 | 793 |

(a) ... $[L+Ga_7Pt_3+GaSb] \rightleftharpoons [L+Ga_7Pt_3]$, (b) ... $[L+Ga_7Pt_3] \rightleftharpoons [L+Ga_7Pt_3+Ga_2Pt]$, (c) ... $[L+Ga_2Pt+Ga_7Pt_3] \rightleftharpoons [L+Ga_2Pt]$.

GaSb–$Ga_7Pt_3$, one might conclude, that the maximum may occur in the three-phase field $[L+GaSb+Ga_2Pt]$ rather than in the three-phase field $[L+GaSb+Ga_7Pt_3]$.

On the other hand, the effect which could only be interpreted as melting of $Ga_7Pt_3$ in the reaction $[L+Ga_2Pt+Ga_7Pt_3] \rightleftharpoons [L+Ga_2Pt]$ (compare Table 4), which was to be expected in the section GaSb–$Ga_7Pt_3$, was also found in the section GaSb–$Ga_2Pt$. In Fig. 6 the following arguments are demonstrated: the three-phase field $[L+Ga_2Pt+Ga_7Pt_3]$ starts in the binary peritectic reaction $L+Ga_2Pt \rightleftharpoons Ga_7Pt_3$ at 822°C. Therefore, the composition of the liquid phase in this three-phase field begins with an antimony content of 0 at.% and the antimony content of L increases subsequently with decreasing temperature (i.e., it follows the liquidus valley). The existence of the three-phase field $[L+Ga_2Pt+Ga_7Pt_3]$ in the section GaSb–$Ga_2Pt$ is only possible, if the composition of the liquid phase lies on the antimony-rich side of this section, because $Ga_7Pt_3$ is situated on the antimony-poor side of the section. In other words, the liquidus valley of $[L+Ga_2Pt+Ga_7Pt_3]$ has to cross the section GaSb–$Ga_2Pt$ (compare Fig. 6). An investigation of the liquidus surface projection shows, that this would not be consistent with a maximum in the three-phase field $[L+GaSb+Ga_2Pt]$.

It is therefore concluded, that a combination of the transition reaction U2: $[L+Ga_7Pt_3 \rightleftharpoons GaSb+Ga_2Pt]$ at 703°C with a temperature maximum in the three-phase field $[L+Ga_7Pt_3+GaSb]$ is the most likely explanation of the experimental results within the two sections GaSb–$Ga_2Pt$ and GaSb–$Ga_7Pt_3$.

### 4.4. Ternary reaction scheme and liquidus surface

By combining the DTA data of series I and series II with the isothermal section at 500°C (Fig. 1) and the available phase diagram information for the limiting binary systems (Table 1), it was possible to construct a complete reaction scheme in the investigated composition area. The Scheil diagram in Fig. 7 shows the occurrence of six invariant ternary reactions, including four transition reactions, one ternary eutectic and one quasibinary eutectic reaction. As an additional feature, a maximum in the three-phase field $[L+Ga_7Pt_3+GaSb]$ had to be introduced

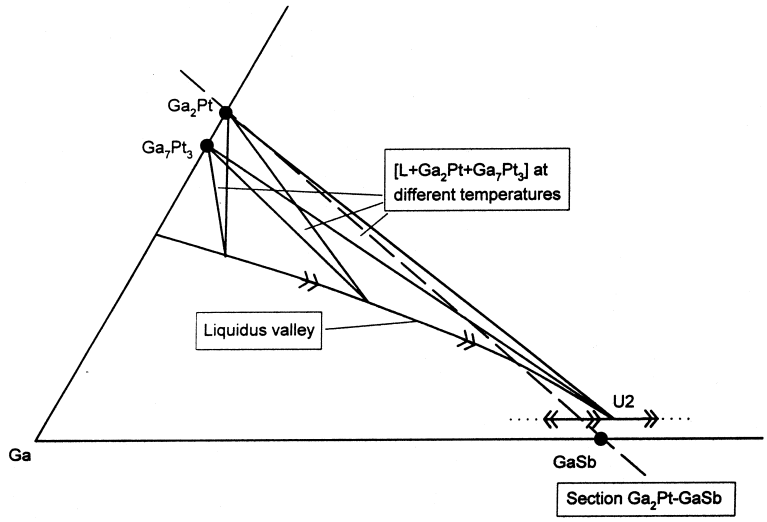


Fig. 6. Course of the liquidus valley $[L+Ga_2Pt+Ga_7Pt_3]$ (Schematic).

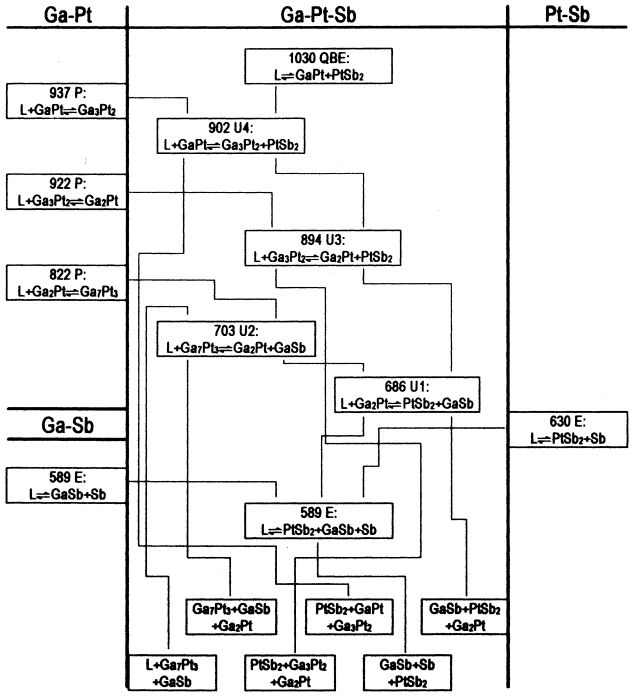


Fig. 7. Scheil diagram for the platinum-poor part of Ga–Pt–Sb.

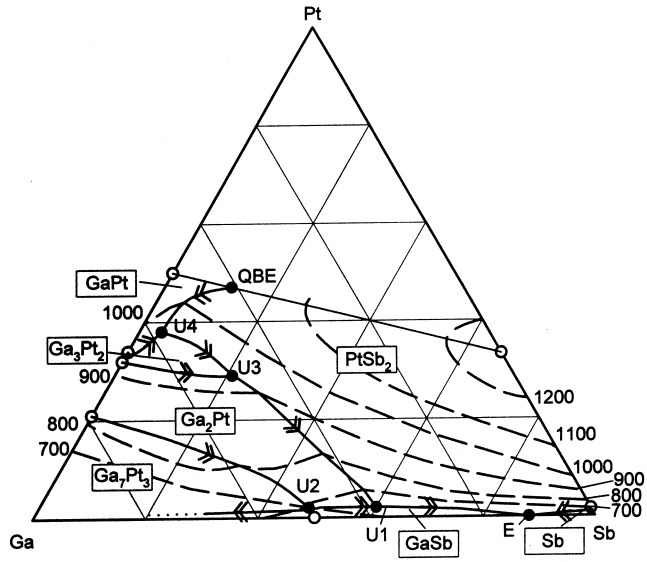


Fig. 8. Liquidus surface projection for Ga–Pt–Sb in the investigated composition range with the fields of primary crystallization. Solid lines ... three phase valleys, dashed lines ... isotherms, ○ ... binary invariant points, ● ... ternary invariant points.

to yield a consistent ternary reaction scheme (see Section 4.3).

The invariant ternary reactions determined in the present study are listed in Table 5. The corresponding equilibrium compositions are based upon EPMA measurements of DTA samples that had been cooled with a cooling rate of 2 K $min^{-1}$. Nevertheless it is thought, that these composition values provide a good approximation of the equilibrium compositions of the phases at the temperatures of the invariant reactions.

All liquidus values from DTA measurements were combined with literature data for the limiting binary systems to yield a liquidus surface projection for the entire investigated composition range. The corresponding diagram in Fig. 8 shows the isotherms between 1200 and 700°C as dashed lines. The liquidus valleys, which separate the different fields of primary crystallization, are shown as solid lines and the fields of primary crystallization are labelled. $PtSb_2$, $Ga_2Pt$ and $Ga_7Pt_3$ show extended fields of primary crystallization, whereas the primary crystallization fields of GaPt and $Ga_3Pt_2$ are rather small. Furthermore, primary crystallization of GaSb and Sb occurs only in a very narrow composition range near the limiting binary Ga–Sb system.

## 5. Conclusions

The Ga–Pt–Sb phase diagram was studied by experimental methods such as DTA, XRD and EPMA in the composition range limited by the binary Ga–Sb system and the section GaPt–$PtSb_2$ with special emphasis being paid to the phase equilibria involving the compound semiconductor GaSb. Five invariant four-phase equilibria and a quasibinary eutectic reaction were identified in the investigated composition area. An isothermal section of the system, which was studied at 500°C, was found to be in perfect agreement with the section given by Markovski et al. [13]. A ternary reaction scheme (Scheil diagram) and a liquidus surface projection were derived from the experimental data.

In the search for suitable metallizations for GaSb, the

Table 5
Invariant ternary reactions in the system Ga–Pt–Sb

| | Phase reaction | Temperature (°C) | | Composition of the involved phases (at.% Ga, Pt, Sb) | | |
|---|---|---|---|---|---|---|
| E: | $L \rightleftharpoons Sb + PtSb_2 + GaSb$ | 589 | L: 12, 0, 88 | Sb: 0, 0, 100[a] | GaSb: 50, 0, 50[a] | $PtSb_2$: 0, 33.3, 66.7[a] |
| U1: | $L + Ga_2Pt \rightleftharpoons GaSb + PtSb_2$ | 686 | L: 38, 2, 60 | $Ga_2Pt$: 65, 32.5, 2.5[a] | GaSb: 50, 0, 50[a] | $PtSb_2$: 0, 33.3, 66.7[a] |
| U2: | $L + Ga_7Pt_3 \rightleftharpoons GaSb + Ga_2Pt$ | 703 | L: 50, 2, 48 | $Ga_2Pt$: 66.5, 32.5, 1[a] | GaSb: 50, 0, 50[a] | $Ga_7Pt_3$: 69.5, 30, 0.5[a] |
| U3: | $L + Ga_3Pt_2 \rightleftharpoons Ga_2Pt + PtSb_2$ | 894 | L: 50, 29, 21 | $Ga_2Pt$: 62.5, 33.5, 4[a] | $Ga_3Pt_2$: 60, 40, 0[a] | $PtSb_2$: 0, 33.3, 66.7[a] |
| U4: | $L + GaPt \rightleftharpoons Ga_3Pt_2 + PtSb_2$ | 902 | L: 58,38, 4 | GaPt: 50, 50, 0[a] | $Ga_3Pt_2$: 60, 40, 0[a] | $PtSb_2$: 0, 33.3, 66.7[a] |
| QBE: | $L \rightleftharpoons GaPt + PtSb_2$ | 1033 | L: 41, 47,12 | GaPt: 50, 50, 0[a] | $PtSb_2$: 0, 33.3, 66.7[a] | |

[a] Composition measured by EPMA (rounded).

three phases that have been found to exist in thermodynamic equilibrium with GaSb, i.e. $Ga_7Pt_3$, $Ga_2Pt$ and $PtSb_2$, may be considered as possible contact materials.

## Acknowledgements

The financial support of the Austrian Fonds zur Förderung der wissenschaftlichen Forschung (Project No. P 10739-CHE) is gratefully acknowledged.

## References

[1] R. Schmid-Fetzer, J. Electron. Mater. 17 (1987) 193.
[2] T. Sands, J. Met. 38 (1986) 31.
[3] T. Sands, Mater. Sci. Eng. B 1 (1989) 289.
[4] R. Beyers, K.B. Kim, R. Sinclair, J. Appl. Phys. 61 (1987) 2195.
[5] K.W. Richter, K. Micke, H. Ipser, Thermochim. Acta, 314 (1998).
[6] K.W. Richter, H. Ipser, Ber. Bunsenges. Phys. Chem., in print (1998).
[7] K.W. Richter, K. Micke, H. Ipser, Mater. Sci. Eng., in print (1998).
[8] K. Micke, S.L. Markovski, H. Ipser, F.J.J. van Loo, Ber. Bunsenges. Phys. Chem., in print (1998).
[9] T.L. Ngai, R.C. Sharma, Y.A. Chang, Bull. Alloy Phase Diagr. 9 (1988) 586.
[10] V.P. Itkin, C.B. Alcock, J. Phase Equilibria 17 (1996) 356.
[11] T.B. Massalski, J.L. Murray, L.H. Bennett, H. Baker (Eds.), Binary Alloy Phase Diagrams, ASM, Materials Park, OH (1990).
[12] P. Guex, P. Feschotte, J. Less-Common Met. 46 (1976) 101.
[13] S.L. Markovski, M.C.L.P. Pleumeekers, A.A. Kodentsov, F.J.J. van Loo, J. Alloys Comp. 268 (1998) 188.
[14] M.E. Straumanis, C.D. Kim, J. Appl. Phys. 36 (1968) 3822.
[15] S. Furuseth, K. Selte, A. Kjekshus, Acta Chem. Scand. 19 (1965) 735.
[16] E. Hellner, F. Laves, Z. Naturforsch. A2 (1947) 177.
[17] E. Zintl, A. Harder, W. Haucke, Z. Phys. Chem. B35 (1937) 354.
[18] K. Schubert, H.L. Lukas, H.G. Meissner, S. Bhan, Z. Metallkd. 50 (1959) 534.